Turk J Chem
34 (2010) , 67 – 79.

doi:10.3906/kim-0903-29

Influence of $AlCl_3$ on the optical properties of new synthesized 3-armed poly(methyl methacrylate) films

Adnan KURT
Department of Chemistry, Faculty of Arts and Science, University of Adıyaman, 02040, Adıyaman-TURKEY
e-mail: adnkurt@gmail.com

Received 11.03.2008

Three-armed poly(methyl methacrylate)[PMMA] was synthesized by atom transfer radical polymerization at 100 °C using benzene-1,3,5-triyl tris(4-(bromomethyl) benzoate as 3-armed initiator and a cuprous(I) bromide/2,2′-bipyridine catalytic system. The characterization of PMMA was confirmed by FT-IR, ^{1}H-NMR, GPC, DSC, and TGA techniques. Optical absorption measurements were also studied by UV-VIS technique. Transmittance and reflectance measured in the wavelength range 300-700 nm were used to calculate the optical constants. The changes in dispersion and Urbach parameters were investigated as a function of $AlCl_3$ content. The wide band tails increased in width and the optical energy gap decreased from 2.39 to 1.28 eV as the $AlCl_3$ content increased from 0% to 15%. Analysis revealed that the type of transition is the indirect allowed one.

Key Words: Optical constants, optical band gap, dispersion parameters, thin films, ATRP, PMMA.

Introduction

The progress of living radical polymerization for the synthesis of polymers with controlled architecture, molecular weight, and molecular weight distribution is among the most important achievements in polymer chemistry in the last 2 decades.[1,2] One of the representative achievements obtained in the area of living radical polymerization should be atom transfer radical polymerization.[3,4] Atom transfer radical polymerization is a living radical polymerization system that has been indicated to successfully polymerize a series of vinyl monomers such as (meth)acrylate, (meth)acrylamide, and styrene as well as its derivative and acrylonitrile.[5–8] ATRP has been shown to be more versatile with respect to the novel polymer architectures such as graft copolymers, block copolymers, and (hyper)branched polymers.[9–11] It is also one of the most effective synthetic methods that can be applied to prepare well-defined polymers with controlled chain topology, composition, microstructure, and

functionality.[2,12–14] The slow growth of polymer chains mediated by fast and reversible activation/deactivation reactions, and the fast initiation process make the polymerization system proceed in a controlled/living form.[15]

The stability of polymer thin films on solid substrates is of great technological importance in applications ranging from protective coatings to paintings, semiconductors, and micro- and optoelectronic devices.[16,17] Optical polymers have attracted considerable attention in recent years because of their important industrial applications. PMMA is one of the earliest and best known polymers. PMMA was seen as a replacement for glass in a variety of applications and is currently used extensively in glazing applications. The material is one of the hardest polymers, and is rigid, glass-clear with glossy finish and good weather resistance. PMMA is naturally transparent and colorless. The transmission for visible light is very high. Polymeric composites of PMMA are known for their importance in technical applications.[18] Studies of doping transition metal halides into PMMA are important for determining and controlling the operational characteristic of the different PMMA composites. The addition of transition metal halides to the PMMA network will cause a remarkable change in their properties.[19] In the study of physical properties of polymers, the optical absorption spectrum is one of the most important tools for understanding band structure, electronic properties, and optical constants (refractive and absorption indices) of pure and doped polymers.

The objective of this study was to synthesize and characterize the 3-armed poly(methyl methacrylate) and to investigate the $AlCl_3$ dependence of some optical properties of polymer films. For this purpose, the Urbach parameters, the optical energy gap, and single-oscillator parameters were evaluated as a function of $AlCl_3$ concentration.

Experimental

Materials

Methyl methacrylate (MMA) was distilled under vacuum after washing with 5% NaOH aqueous solution just before polymerization. Cuprous(I) bromide (CuBr), 2,2′-bipyridine, diphenyl ether, dichloromethane, methanol, and trihydroxybenzene (analytical reagent) were used as received. The benzene-1,3,5-triyl tris(4-(bromomethyl) benzoate used as initiator for ATRP was synthesized in the laboratory.

Instrumental techniques

UV-visible spectrums of the thin films were recorded by a T80 + UV/VIS Spectrometer (PG Instruments Ltd.) in the wavelength range 300-700 nm at room temperature. Gel permeation chromatography (GPC) analyses were carried out using a high pressure liquid chromatography pump with an Agilent 1100 system equipped with a vacuum degasser and a refractive index detector. The eluting solvent was tetrahydrofuran (THF) and the flow rate was 1 mL min^{-1}. Calibration was achieved with polystyrene. Thermogravimetric analysis (TGA) and differential scanning calorimetry (DSC) measurements were carried out using a Shimadzu TGA-50 and DSC-50 under nitrogen flow with heating rate of 10 and 20 °C min^{-1}, respectively. Infrared spectra were recorded on a Perkin Elmer Spectrum One and obtained by polymer film on a salt plate. ^{1}H-NMR spectra were recorded on a Bruker AC-300 MHz Fourier Transform NMR spectrometer at room temperature using $CDCl_3$ as a solvent and TMS as an internal standard. The films of the 3-armed PMMA polymer were prepared by the solution

casting method.[20] In this method, the polymer is dissolved in a suitable solvent and poured onto a flat, carefully cleaned substrate, and then the solvent evaporates from a solution of the polymer samples. For this purpose, the dichloromethane solvent, (CH_2Cl_2), pro analysis, from Merck, was used to produce polymer films. Before being used as substrates, the glass disks, with a thickness of 1.27 mm, a length of 80.20 mm, and a width of 23.22 mm, were carefully washed with detergent and afterwards with ethyl alcohol vapors and dried in a vacuum oven at room temperature. Several drops of the polymer solution (the concentration, PMMA/dichloromethane = 50 mg/mL) were poured onto the substrate. To avoid thermal gradients and minimize the effect of the evaporation of the solvent immediately after deposition, both the polymer solution and the substrates were kept at the same temperature and an evaporation barrier was placed on the substrates. The polymer films were placed in a vacuum oven at room temperature, for 5 h. Afterwards, the temperature of the oven was gradually raised to a value slightly under the glass transition temperature of the PMMA, 100 °C, in order to remove completely any residual solvent. The films were kept at this temperature for 1 day. After being cooled down slowly, the films were stored at room temperature. The thicknesses of the films were adjusted to 200 nm for pure and doped polymers. The optical parameters of pure and doped films were calculated according to the methods given in the literature.[21–26]

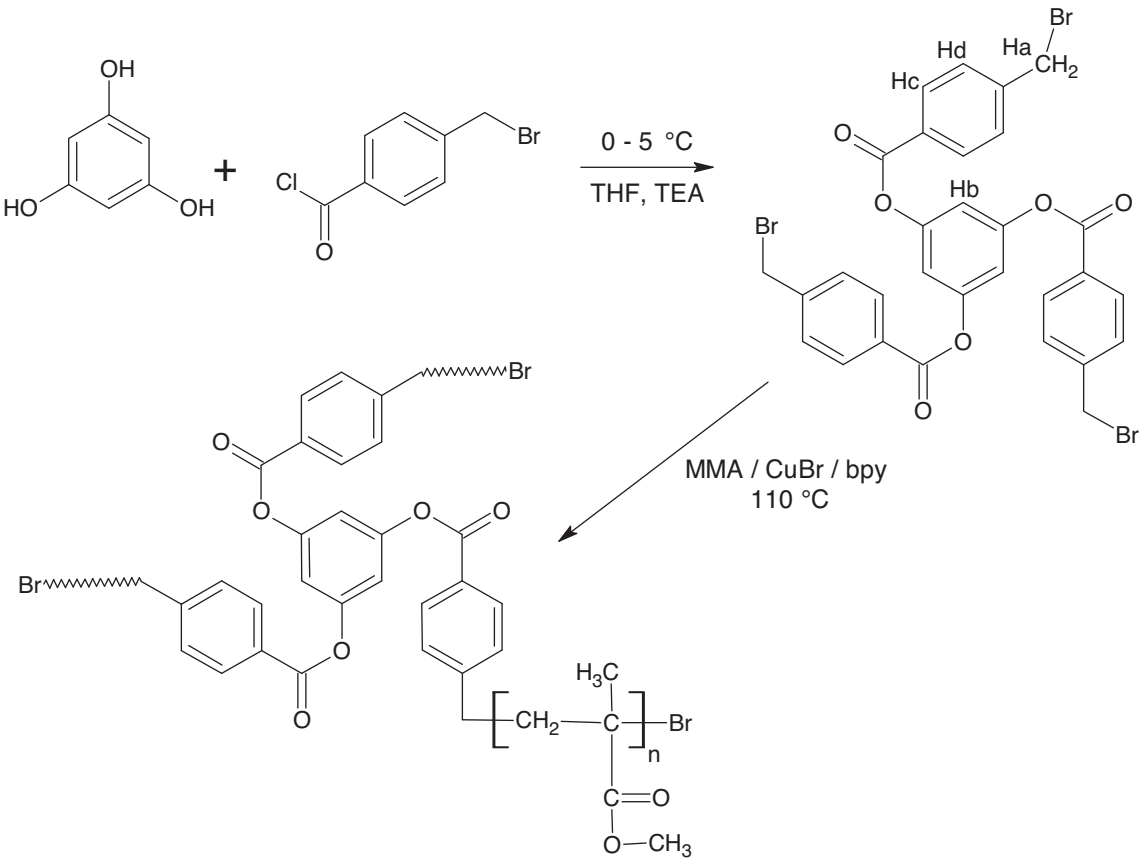

Scheme. Synthesis of 3-armed PMMA.

Synthesis of benzene-1,3,5-triyl tris(4-(bromomethyl) benzoate

The synthesis and characterization of benzene-1,3,5-triyl tris(4-(bromomethyl) benzoate were as described in the literature.[27] This synthesis was accomplished with the reaction of 2-bromobenzoyl chloride (0.3 mol) with trihydroxybenzene (0.1 mol) between 0 and 5 °C using triethylamine (0.31 mol) and tetrahydrofuran (100 mL), and then it was crystallized from methanol.

Atom transfer radical polymerization of MMA

A typical procedure for the ATRP synthesis of MMA is as follows: deoxygenated CuBr (0.01 g), 2,2′-bipyridine (0.022 g), and tri-drops diphenyl ether were added to a dried glass tube to produce ATRP complex. Benzene-1,3,5-triyl tris(4-(bromomethyl) benzoate (0.0165 g) as 3-armed initiator and then MMA (0.7 g) were added to this deep brown mixture under argon atmosphere. The glass tube was then closed with a rubber septum and immersed in a preheated oil bath at 100 °C. The polymerization was continued for 4 h. The polymerization mixture was then diluted with dichloromethane, filtered, and poured into excess ethyl alcohol with 1% aqueous hydrochloric acid. The polymer so purified was isolated and dried in a vacuum oven at 45 °C for 24 h. The polymer yield was calculated gravimetrically.

Results and discussion

Atom transfer radical polymerization of 3-armed PMMA was carried out using an initiator with tri-active C-Br end group function and cuprous(I) bromide/2,2′-bipyridine catalytic system in the molar ratio of 1:3:6:300 for 3 armed initiator: Cu(I)Br:bpy:MMA, respectively.[28–30] The schematic representation of polymer synthesis is illustrated in Scheme 1. Figure 1a shows the FT-IR spectra of benzene-1,3,5-triyl tris(4-(bromomethyl) benzoate. The characteristic bands are assigned to C-H stretching of the aromatic ring at 3126-3038 cm^{-1}, aliphatic C-H stretching at 2967-2868 cm^{-1}, C=O stretching vibration at 1739 cm^{-1}, and aromatic ring C=C stretching vibration at 1610 cm^{-1}.

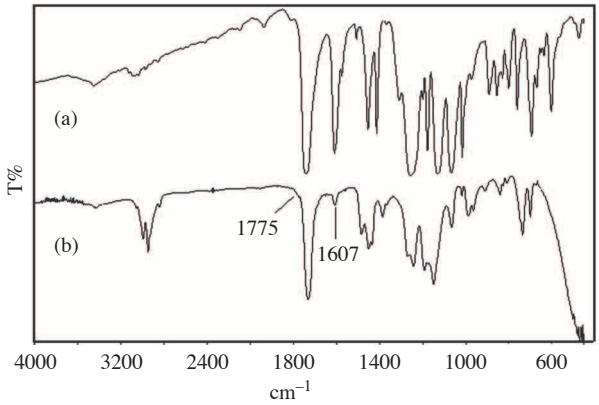

Figure 1. FT-IR spectra of (a) benzene-1,3,5-triyl tris(4-(bromomethyl) benzoate and (b) 3-armed PMMA.

The ^{1}H-NMR spectra of benzene-1,3,5-triyl tris(4-(bromomethyl) benzoate are illustrated in Figure 2a. The signals at 8.2 ppm (proton integrals = 4.56) and 7.5 ppm (proton integrals = 4.56) are attributed to aromatic

ring protons next to ester carbonyl (H_c) and next to bromine methyl (H_d), respectively. The aromatic ring protons in the core (H_b) are shown at 7.2 ppm (proton integrals = 2.29). The signal attributed to bromine methyl protons is also shown at 4.6 ppm (proton integrals = 4.58). Figure 1b shows the FT-IR spectra for 3-armed PMMA. The bands at 3054-3005 cm^{-1} and 2925-2846 cm^{-1} are assigned to aromatic (from initiator units) and aliphatic C-H stretching, respectively. The small peaks at 1775 cm^{-1} and 1607 cm^{-1} are also attributed to ester carbonyl and aromatic ring C=C stretching reasoned from 3-armed initiator. The strong peak at 1730 cm^{-1} is characteristic for ester carbonyl in MMA units. Figure 2b shows the ^{1}H-NMR spectra of PMMA in which the signals at 1.95-1.2 ppm are assigned to the CH_3 and CH_2 protons in the main chain. The signal at 3.67 ppm is characteristic for CH_3 protons next to ester carbonyl in MMA units. The very small signals seen at ≈7-8 ppm are attributed to aromatic ring protons reasoned from the 3-armed initiator unit on the head of polymer chains.

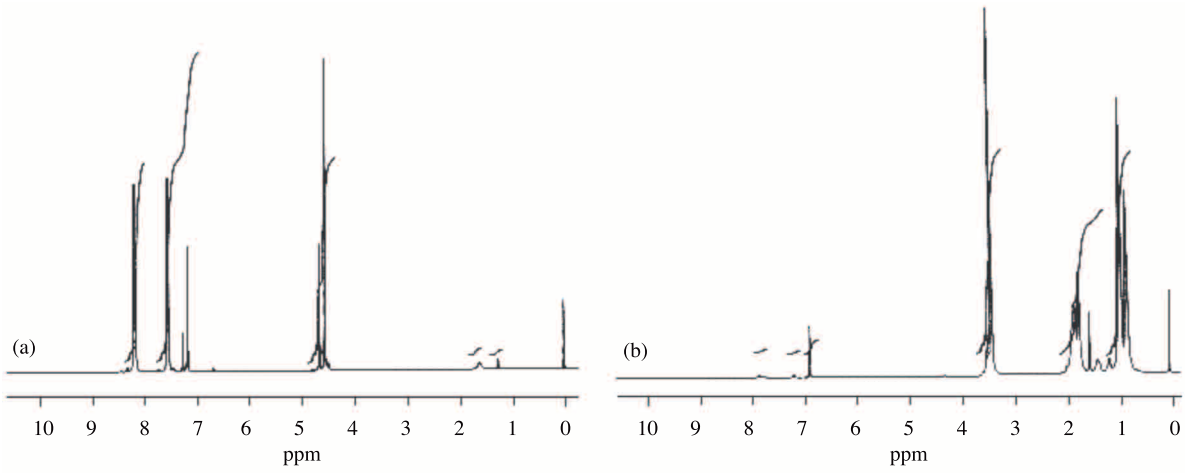

Figure 2. ^{1}H-NMR spectra of (a) benzene-1,3,5-triyl tris(4-(bromomethyl) benzoate and (b) 3-armed PMMA.

The theoretical number-average molecular weight was calculated according to the relation $M_{n,theo} = ([M]_0/[I]_0) \times$ conversion $\times$ $MW_{mon} + MW_{init}$, where $[M]_0$ and $[I]_0$ are initial concentrations of monomer and initiator, while MW_{mon} and MW_{init} are molecular weights of monomer and initiator, respectively. Theoretical number-average molecular weight for purified 3-armed PMMA at 82% monomer conversion was calculated as $M_{n,theo}$ = 25,300 using the above relation. The molecular weight of polymer was also determined according to ^{1}H-NMR. The signals of the chemical shifts at 7-8 ppm (sum of aromatic proton integrals = 1.12) correspond to the aromatic ring protons from the 3-armed initiator unit on the head of polymer chains and the chemical shifts at 3.67 ppm (proton integrals = 46.8) correspond to the CH_3 protons next to ester carbonyl in MMA units and can be used as the internal standard to calculate the molecular weight. The number of repeating monomer units was estimated from the ratio of integral peak areas of CH_3 protons to that of the aromatic ring protons. Thus, molecular weight determined by ^{1}H-NMR technique was calculated as $M_{n,NMR}$ = 21,250. When the number-average molecular weight of the purified polymer was measured on a gel permeation chromatography (GPC) system, this value was determined as $M_{n,GPC}$ = 14,250 and molecular weight distribution was 2.1. While the M_n measured with the GPC system is close to that of the NMR system, this value does not agree with the theoretical prediction of $M_{n,theo}$ = 25,300. For a controlled/"living" polymerization the observed

molecular weight should coincide with the theoretical relation. A discrepancy between observed and theoretical molecular weights indicates a transfer reaction to some low molecular weight species.[31] Here, polydispersity was partially observed at a high value due to the variable quantity of initiating sites per chain. The high value in the molecular weight distribution for the MMA polymerization may have originated from slow ATRP initiation of MMA from the primary alkyl halide sites in the 3-armed initiator. It can also be caused by deactivation of chain ends and termination reactions that are more evident at higher monomer conversion.[32]

The glass transition temperature value (Figure 3) was 116 °C at a heating rate of 20 °C/min for pure 3-armed PMMA. The decomposition of pure 3-armed PMMA obtained from ambient temperature to 500 °C at a heating rate of 10 °C/min under nitrogen flow occurs in a single step at about 291 °C, and its thermogram is shown in Figure 4. The residue at 450 °C was 2%.

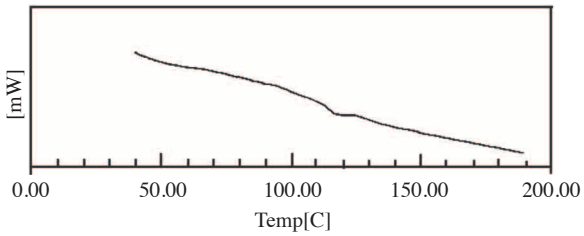

Figure 3. DSC curve of 3-armed PMMA at a heating rate of 20 °C/min.

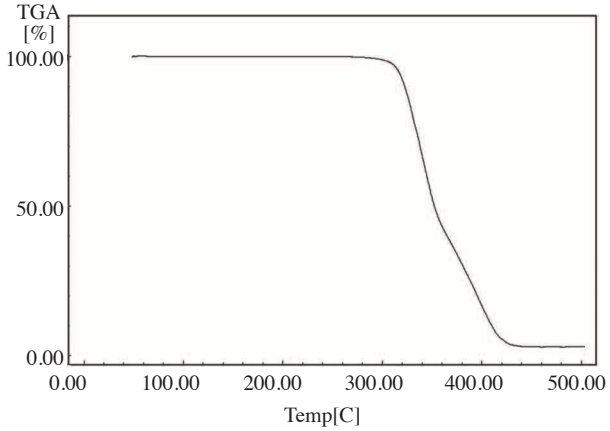

Figure 4. TGA curve of 3-armed PMMA at a heating rate of 10 °C/min.

The optical absorption measurements were carried out in the UV/VIS region (300-700 nm) for films of 3-armed PMMA and doped with different contents of $AlCl_3$. The absorption spectra at about 300 nm of pure and doped PMMA films may be attributed to n-π^* transition of the carbonyl group in the polymeric macromolecule.[21] The transmittance and reflectance of pure and doped PMMA polymer films recorded in the applied wavelength range are shown in Figure 5. It is clear from this figure that transmittance spectra for all films increased with increasing wavelength while reflectance decreased. Increasing the $AlCl_3$ content of the films decreases transmittance and increases reflectance for a lower wavelength range. This means that there is some absorption in that wavelength range. For each composition typical spectral behavior of transmittance and reflectance are given for pure and doped PMMA films.

The refractive index, $n(\lambda)$, was determined from the absolute values of the transmittance and reflectance of the investigated films using the following formula:[22,33]

$$n = \left[\frac{1+R}{1-R}\right] + \left[\frac{4R}{(1-R)^2} - k^2\right]^{1/2} \tag{1}$$

where k is the extinction coefficient and R is the optical reflectance. The extinction coefficient can be obtained from the relation where $k = \alpha\lambda/4\pi$. Plots in Figure 6 represent the dispersion in the refractive index for pure

and doped PMMA thin films in the investigated range of wavelengths. Inspection of Figure 6 indicates for all compositions that the refractive index decreases with increasing wavelength as well as it increases as $AlCl_3$ content increases from 0% to 15%. The values of the refractive index at 300 nm and room temperature for 0%, 5%, 10%, and 15% $AlCl_3$ content were 4.10; 4.56; 4.77; and 5.04, and at 700 nm they were 1.83; 2.14; 2.22, and 2.37, respectively. Among these contents, the magnitude of the refractive index of 15% $AlCl_3$ content has the highest value (n = 5.04 at 300 nm). A more rapid decrease in n values may be seen at the low wavelength range 300-450 nm. Towards a higher wavelength range, the decrease in the n values is slower and reaches a nearly constant value.

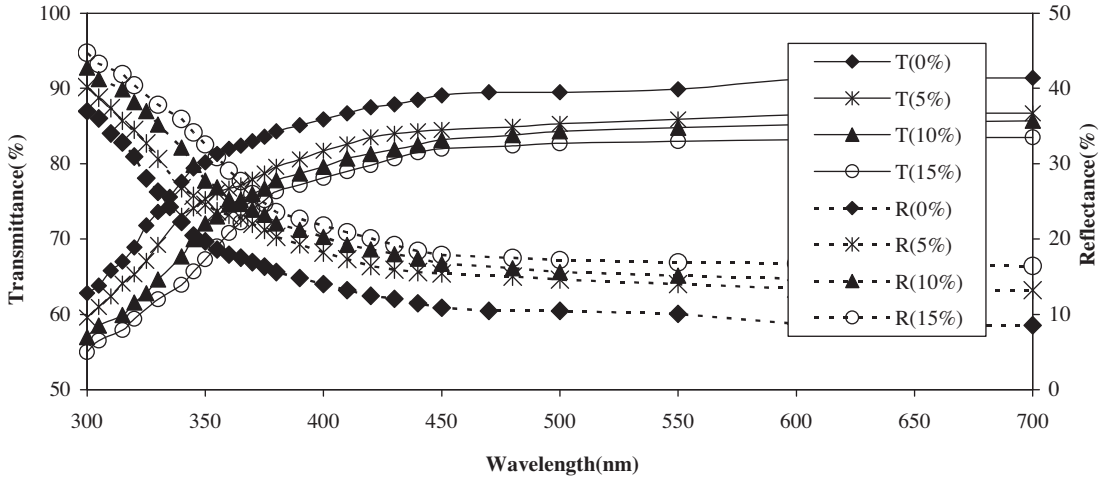

Figure 5. The transmittance and reflectance spectra of films.

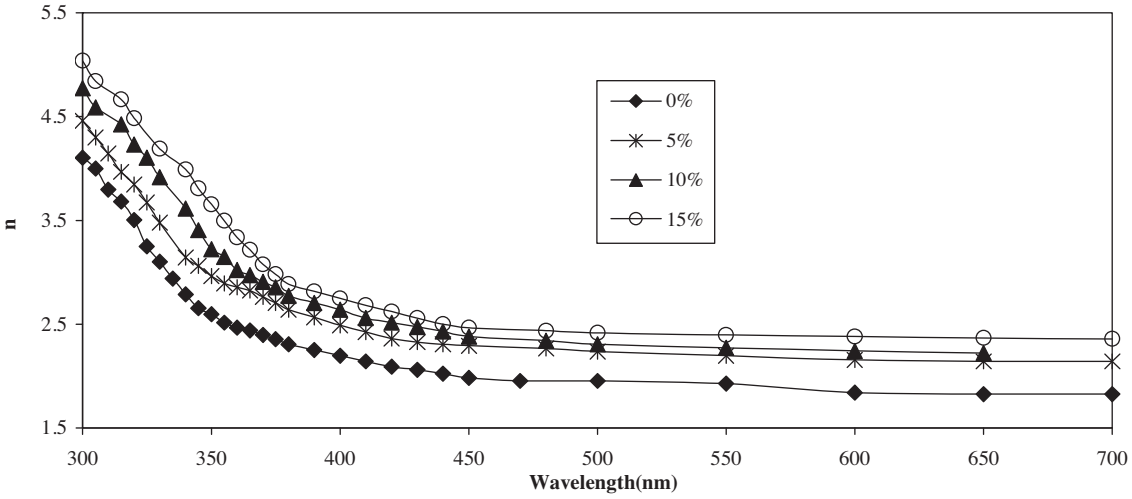

Figure 6. The refractive index dispersion curves of films.

The real ε_r and imaginary ε_i parts of the dielectric constant were obtained using the formula $\varepsilon_r = n^2 - k^2$ and $\varepsilon_i = 2nk$. The variation in the real (ε_r) and imaginary (ε_i) parts of the dielectric constant for different $AlCl_3$ contents are shown in Figure 7 (a, b). The values of the real part are higher than those of the imaginary

part. The values of real and imaginary parts of the dielectric constant at 2 eV for 0%, 5%, 10%, and 15% $AlCl_3$ content were 3.34; 4.58; 4.94; and 5.60 and 0.084; 0.157; 0.178, and 0.220, respectively.

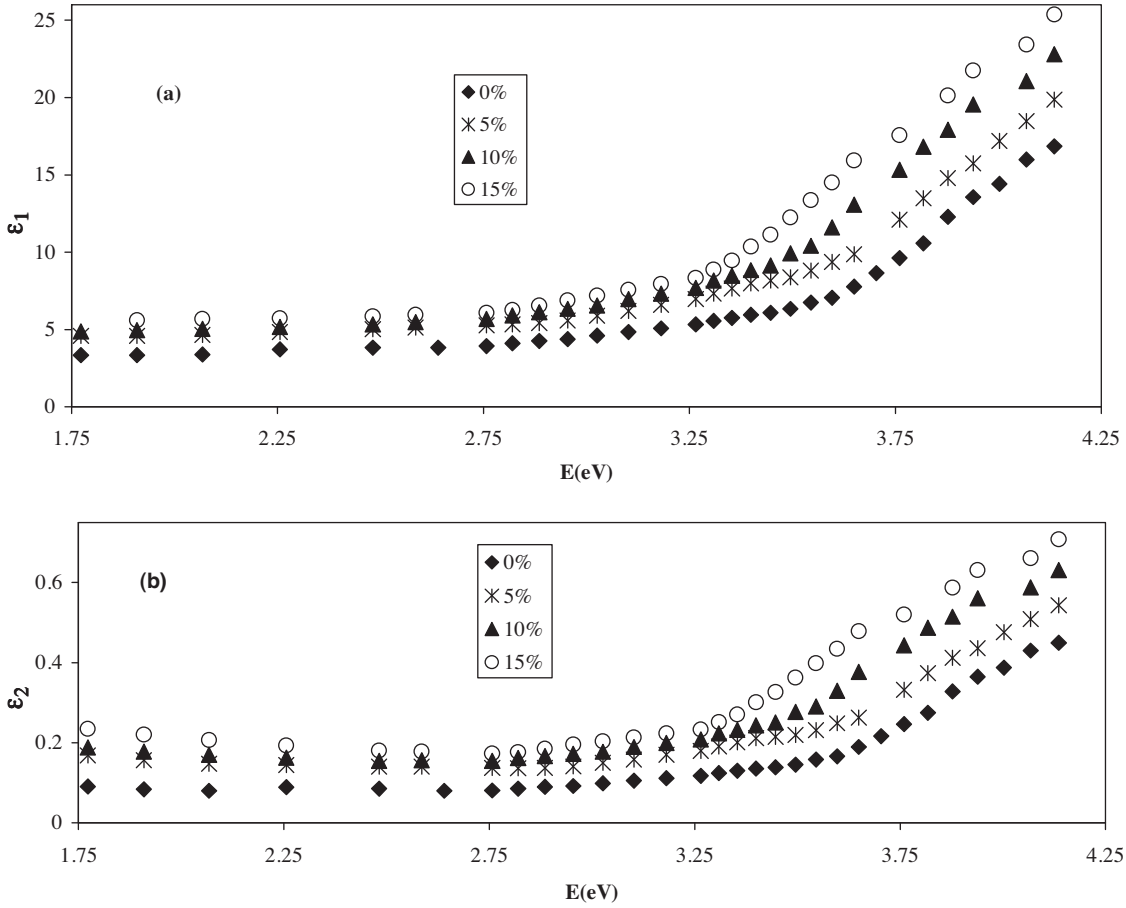

Figure 7. The spectra of real (a) and imaginary (b) parts of the dielectric constant of films.

The refractive index dispersion data were evaluated according to the single-effective-oscillator model[34,35] using the following relation:

$$n^2(h\nu) = 1 + \frac{E_o E_d}{E_o^2 - (h\nu)^2} \tag{2}$$

The physical meaning of the single-oscillator energy E_o is that it simulates all the electronic excitation involved and E_d is the dispersion energy related to the average strength of the optical transitions.[23] In practice the dispersion parameters E_d and E_o can be obtained according to Eq. (2) by a simple plot of $(n^2 - 1)^{-1}$ versus $(h\nu)^2$ as shown in Figure 8. The values of E_d and E_o can be directly determined from the slope and the intercept on the vertical axis. The values obtained for the dispersion parameters E_o and E_d are listed in the Table. The values of E_o and E_d for 0%, 5%, 10%, and 15% $AlCl_3$ content were 4.24; 4.21; 4.03; and 4.20 eV, and 7.42; 9.98; 10.78, and 11.29 eV, respectively. According to the single-oscillator model, the single oscillator parameters E_o and E_d are related to the imaginary part of the complex dielectric constant; the moments of

the imaginary part of the optical spectrum M_{-1} and M_{-3} moments[34,36] can be derived from the following relations and are given in the Table:

$$E_o^2 = \frac{M_{-1}}{M_{-3}}, \quad E_d^2 = \frac{M_{-1}^3}{M_{-3}} \tag{3}$$

For the definition of the dependence of the refractive index n on the light wavelength (λ), the single-term Sellmeier relation can be used:[37]

$$n^2(\lambda) - 1 = \frac{S_o.\lambda_o^2}{1 - (\lambda_o/\lambda)^2} \tag{4}$$

where λ_o is the average oscillator position and S_o is the average oscillator strength. The parameters S_o and λ_o in Eq. (4) can be obtained experimentally by plotting $(n^2 - 1)^{-1}$ against λ^{-2}. From Figure 9, the slope of the resulting straight line gives $1/S_o$, and the infinite-wavelength intercept gives $1/(S_o\lambda_o^2)$. These values can be seen in the Table.

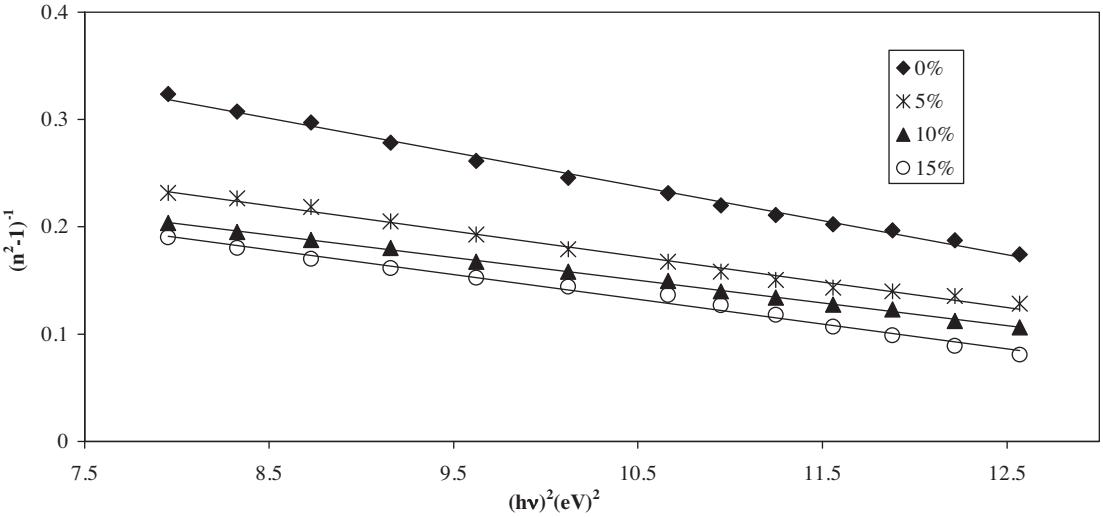

Figure 8. Variation in $(n^2 - 1)^{-1}$ as a function of $(h\upsilon)^2$ of films.

Table. Optical parameters of 3-armed PMMA thin films.

$AlCl_3$ (%wt)	E_o(eV)	E_d(eV)	$S_o.10^{13}(m^{-2})$	λ_o(nm)	M_{-1}	$M_{-3}(eV)^{-2}$	E_t(eV)	σ	E_g(eV)
0	4.24	7.42	2.04	292.79	1.75	0.097	1.252	0.0205	2.39
5	4.21	9.98	2.73	294.46	2.37	0.134	1.407	0.0183	2.02
10	4.03	10.78	2.82	295.63	2.67	0.165	1.485	0.0173	1.52
15	4.20	11.29	3.07	307.77	2.69	0.152	1.597	0.0161	1.28

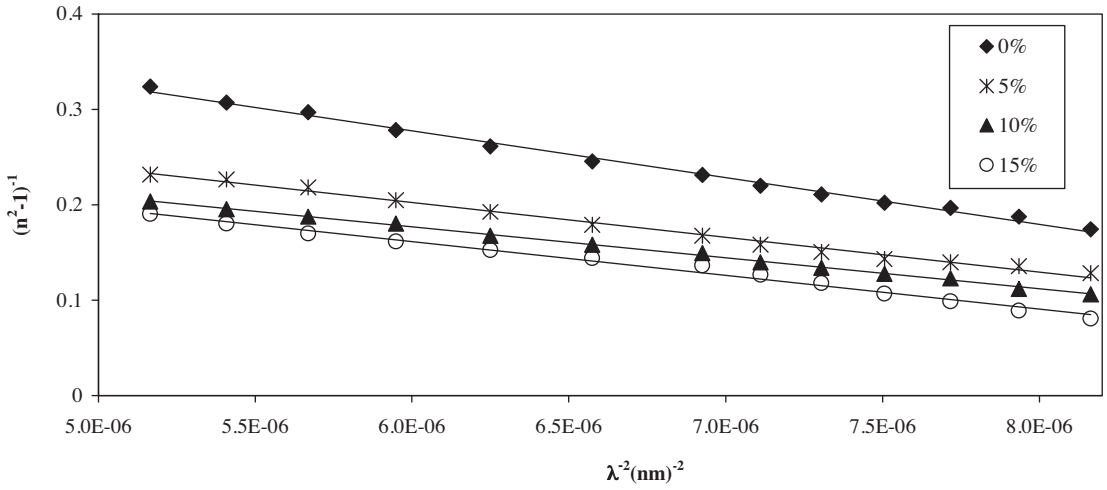

Figure 9. Variation in $(n^2 - 1)^{-1}$ as a function of $(\lambda)^{-2}$ of films.

In the high absorption region (where absorption is associated with interband transitions), the absorption coefficient, α, can be calculated from observed absorbance data using Beer Lambert's formula: $\alpha = 2.303A/d$, where A is the optical absorbance and d is the thickness of the film. It is usual to analyze the optical absorption at the fundamental edge in terms of band-to-band transitions theory in polymers.[38] In this treatment, the absorption data follow a power law, which is given by[39]

$$(\alpha h\nu)^m = g(h\nu - E_g) \tag{5}$$

and yield values of the optical energy band (E_g). Here $g$is a constant and $m$is the power that characterizes the transition process and it can take values such as 2, 1/2, 1/3, or 3/2. The investigation of the spectrum of the absorption coefficient in the fundamental region and near the fundamental edge provides us with valuable information about the energy band structure of the material.[23] The experimental data were fitted to the theoretical Eq. (5) for different values of m and the best fit was obtained for m = 1/2. This behavior indicated that the transitions are allowed indirect transitions.

Plots of $(\alpha h\nu)^{1/2}$ versus the photon energy $(h\nu)$ are shown in Figure 10 in order to achieve the band gap for thin films. The values of the energy gap for each composition were calculated by extrapolating the straight portion to zero absorption. The band gap of the PMMA films decreases with the increase in $AlCl_3$ content from 0% to 15%. The variations in optical band gap with different $AlCl_3$ contents are shown in the Table. The E_g values of films were 2.39; 2.02; 1.52; and 1.28 eV, respectively. This decrease in band gap may be attributed to the presence of unstructured defects, which increase the density of localized states in the band gap and consequently decrease the energy gap.[40]

The tail of the absorption edge is exponential, indicating the presence of localized states in the energy band gap. The amount of tailing can be predicted to a first approximation by plotting the absorption edge data in terms of an equation originally given by Urbach.[41] The absorption edge of non-metallic materials gives a measure of the energy band gap and the exponential dependence of the absorption coefficient, $\ln(\alpha)$, on photon energy, $h\nu$, is found to hold over several decades for a polymeric material and takes the following form:[41]

$$\alpha = \alpha_0 \exp(h\nu/E_t) \tag{6}$$

where α_0 is a constant and E_t is interpreted as the width of the tails of localized states in the gap region. To evaluate the values of α_0 and E_t, it was α in logarithmic scale as a function of photon energy $h\nu$ as shown in Figure 11. The reciprocal of the slope of each line yields the magnitude of E_t and its values for different $AlCl_3$ content of films are listed in the Table. It is clear that $AlCl_3$ dopant increases the width of the tail of localized states and decreases the energy gap of PMMA thin films. Using Eq. (6) at a constant temperature graph representing $\ln(\alpha)$ on the y-axis and $h\nu$ on the x-axis in the range of the Urbach tail would yield a straight line with a slope equal to σ/kT, where σ, known as the steepness parameter, is a temperature-dependent parameter characterizing the broadening of the absorption edge due to electron–phonon or exciton–phonon interactions,[26,42] k is the Boltzmann constant, and T is the temperature. If temperature is taken as 298 K, the steepness parameters for 0%, 5%, 10%, and 15% $AlCl_3$ content can be calculated as 0.0205, 0.0183, 0.0173, and 0.0161, respectively. These values can be seen in the Table.

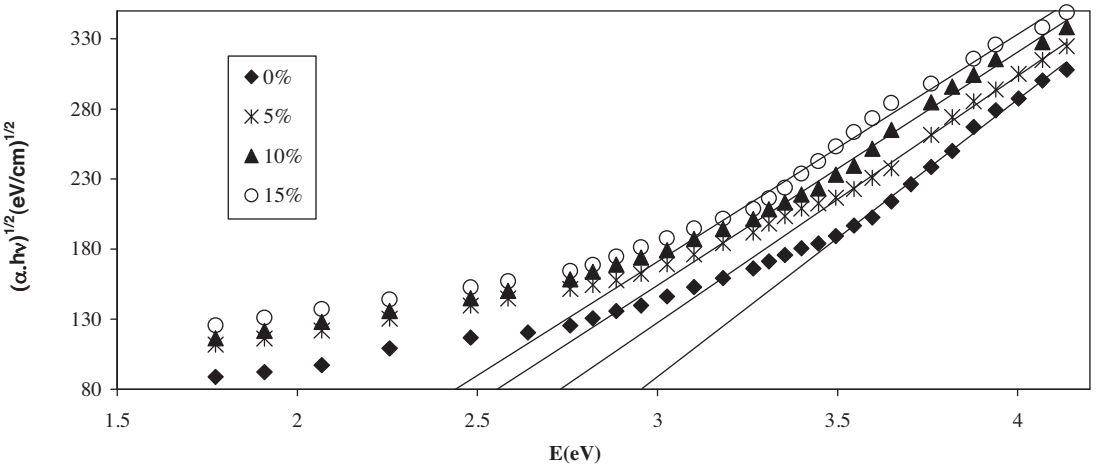

Figure 10. Plots of $(\alpha \mathrm{h}\nu)^{1/2}$ vs. E of films.

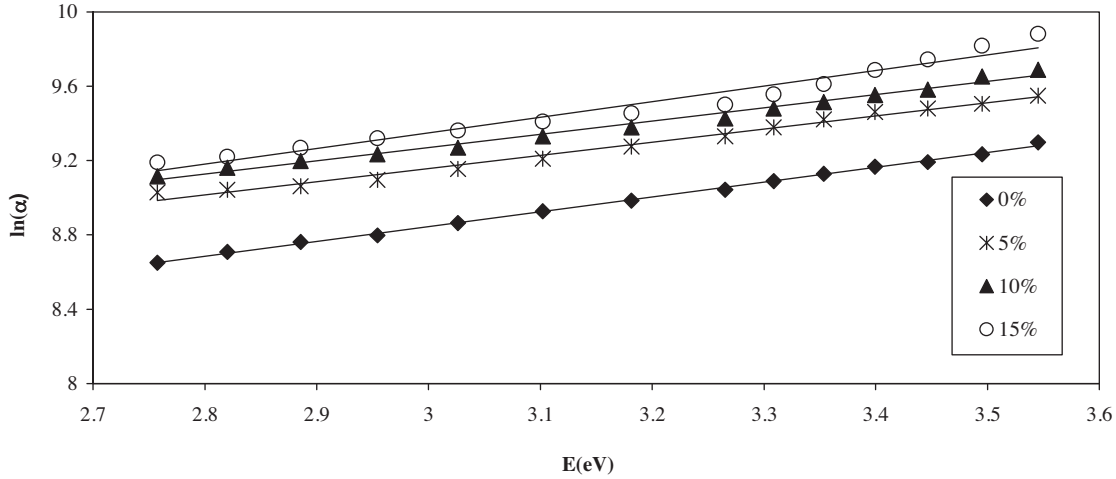

Figure 11. Plots of $\ln\alpha$ vs. E of films.

Conclusions

Three-armed poly(methyl methacrylate)[PMMA] was synthesized by atom transfer radical polymerization at 100 °C using benzene-1,3,5-triyl tris(4-(bromomethyl) benzoate as 3-armed initiator and a cuprous(I) bromide/2,2′-bipyridine catalytic system. The characterization of PMMA was confirmed with FT-IR, ^{1}H-NMR, GPC, DSC, and TGA techniques. The optical absorption measurements were carried out in the UV/VIS region (300-700 nm) for films of 3-armed PMMA and doped with different contents of $AlCl_3$. It was determined that transmittance spectra for all films increased with increasing wavelength while reflectance decreased. The refractive index decreased with increasing wavelength and it increased as $AlCl_3$ content increased from 0% to 15%. The value of refractive index at 300 nm and room temperature for 0%, 5%, 10%, and 15% $AlCl_3$ content were 4.10; 4.56; 4.77; and 5.04, and at 700 nm the values were 1.83; 2.14; 2.22, and 2.37, respectively. The values of the real part were higher than those of the imaginary part. The single–oscillator parameters were determined. The change in dispersion and Urbach parameters were investigated as a function of $AlCl_3$ content. The wide band tails increased in width and optical energy gap decreased from 2.39 to 1.28 eV as the $AlCl_3$ content increased from 0% to 15%. Analysis revealed that the type of transition is the indirect allowed one.

References

1. Hawker, C. J.; Bosman, A. W.; Harth, E. *Chem. Rev.* **2001,** *101,* 3661-3688.
2. Matyjaszewski, K.; Xia, J. H. *Chem. Rev.* **2001,** *101,* 2921-2990.
3. Wang, J. S.; Matyjaszewski, K. *J. Am. Chem. Soc.* **1995**, *117*, 5614-5615.
4. Kato, M.; Kamigaito, M.; Sawamoto, M.; Higashimura, T. *Macromolecules* **1995**, *28*, 1721-1723.
5. Granel, C.; Dubois, P.; Jerome, R.; Teyssie, P. *Macromolecules* **1996,** *29*, 8576-8582.
6. Teodorescu, M.; Matyjaszewski, K. *Macromolecules* **1999,** *32,* 4826-4831.
7. Matyjaszewski, K.; Patten, T. E.; Xia, J. H. *J. Am. Chem. Soc.* **1997**, *119*, 674-680.
8. Matyjaszewski, K.; Jo, S. M.; Paik, H. J.; Shipp, D. A. Macromolecules **1999,** *32*, 6431-6438.
9. Beers, K. L.; Gaynor, S. G.; Matyjaszewski, K. *Macromolecules* **1998,** *31,* 9413-9415.
10. Demirelli, K.; Kurt, A.; Coskun, M. *Polym-Plast. Techn. Eng.* **2004,** *43,* 1245-1265.
11. Gaynor, S. G.; Edelman, S.; Matyjaszewski, K. *Macromolecules* **1996,** *29*, 1079-1081.
12. Kamigaito, M.; Ando, T.; Sawamoto, M. *Chem. Rev.* **2001,** *101*, 3689-3746.
13. Patten, T. E.; Matyjaszewski, K. *Acc. Chem. Res.* **1999,** *32,* 895-903.
14. Bibiao J.; Jianbo, F.; Yang, Y.; Qiang, R.; Wenyun, W.; Jianjun, H. *Eur. Polym. J.* **2006,** *42*, 179-187.
15. Yu, Q.; Qin, Z.; Li, J.; Zhu, S.; *Polym. Eng. Sci.* **2008,** *48,* 1254-1260.
16. Oslanec, R.; Costa, A. C.; Composto, R. J. *Macromolecules* **2000,** *33*, 5505-5512.
17. Reiter, G. Macromolecules **1994,** *27,* 3046-3052.
18. Tawansi, A.; Zidan, H. M. *Int. J. Polym. Mater.* **1991,** *15*, 77-83.
19. Tawansi, A.; El-Khodary, A.; Zidan, H. M.; Badr, S. I. *Polym. Test.* **2002,** *21*, 381-387.

20. Adao, M. H.; Fernandes, A. C.; Saramago, B.; Cazabat, A. M. *Colloid. Surface. A.* **1998**, *132,* 181-192.
21. Zidan, H. M.; Abu-Elnader, M. *Physica B* **2005,** *355*, 308-317.
22. Islam, M. R.; Podder, J. *Cryst. Res. Technol.* **2009,** *44,* 286-292.
23. Atyia, H. E.;. *Optoelectron. Adv. M.* **2006,** *8,* 1359-1366.
24. Papazoglou, D. G.; Apostolidis, A. G.; Vanidhis, E. D. *Appl. Phys. B* **1997,** *65,* 499-503.
25. El-Nahass, M. M.; Zeyada, H. M.; Abd-El-Rahman, K. F.; Farag, A. A. M.; Darwish, A. A. A. *Spectrochim. Acta. A* **2008,** *69,* 205-210.
26. Abu El-Fadl, A.; Soltan, A. S.; Shaalan, N. M. *Opt. Laser Technol.* **2007,** *39,* 1310-1318.
27. Kurt, A.; Demirelli, K. *Polym. Eng. Sci.* **2010,** *50*, 268-277.
28. Matyjaszewski, K.; Pyun, J.; Gaynor, S. G. *Macromol. Rapid. Commun.* **1998,** *19*, 665-670.
29. Demirelli, K.; Kurt, A.; Coskun, M. *Eur. Polym. J.* **2004,** *40*, 451-457.
30. Demirelli, K.; Kurt, A.; Coskun, M. F.; Coskun, M. *J. Macromol. Sci. A.* **2006**, *43*, 573-587.
31. Matyjaszewski, K.; Miller, P. J.; Pyun, J.; Kickelbick, G.; Diamanti, S. *Macromolecules* **1999,** *32,* 6526-6535.
32. Durmaz, Y.Y.; Karagoz, B.; Bicak, N.; Yagci, Y. *Polym. Int.* **2008,** *57,* 1182-1187.
33. Taue, J**.** *Optical Properties of Solids***;** Abeles**,** F**.** Ed**.;** North**-**Holland**,** Amsterdam, 1972.
34. Wemple, S. H.; DiDomenico, M. *Phys. Rev.* **1971,** *B3*, 1338-1351.
35. Wemple, S. H. *Phys. Rev.* **1973***, B7,* 3767-3777.
36. Ammar, A. H. *Appl. Surf. Sci.* **2002,** *201,* 9-19.
37. Wemple, S. H.; DiDomenico, M. *J. Appl. Phys.* **1969,** *40 ,* 720-734.
38. El-Nahass, M. M.; Abd-El-Rahman, K. F.; Farag, A. A. M.; Darwish, A. A. A.; *Int. J. Modern Phys. B* **2004,** *18*, 421-434.
39. Tauc, J. *Amorphous and Liquid Semiconductors*, Plenum Press, New York, 1974.
40. El-Zahed, H.; El-Korashy, A.; Rahem, M. A. *Vacuum*, **2002,** *68,* 19-27.
41. Urbach, F. *Phys. Rev.* **1953,** *92*, 1324-1330.
42. Mahr, H. *Phys. Rev.* **1962,** *125,* 1510-1516.